Structural basis of myosin V Rab GTPase-dependent cargo recognition

Olena Pylypenko[a,b,1], Wikayatou Attanda[a,b], Charles Gauquelin[a,b], Marion Lahmani[a,b], Doudouh Coulibaly[a,b], Bruno Baron[c,d], Sylviane Hoos[c,d], Margaret A. Titus[e], Patrick England[c,d], and Anne M. Houdusse[a,b,1]

[a]Structural Motility, Institut Curie, 75248 Paris Cedex 05, France; [b]Centre National de la Recherche Scientifique (CNRS), Unité Mixte de Recherche (UMR) 144; [c]Biophysics of Macromolecules and their Interactions, Proteopole, Department of Structural Biology and Chemistry, Institut Pasteur; [d]CNRS, UMR 3528; and [e]Department of Genetics, Cell Biology and Development, University of Minnesota, Minneapolis, MN 55455

Edited* by James A. Spudich, Stanford University School of Medicine, Stanford, CA, and approved October 23, 2013 (received for review July 29, 2013)

Specific recognition of the cargo that molecular motors transport or tether to cytoskeleton tracks allows them to perform precise cellular functions at particular times and positions in cells. However, very little is known about how evolution has favored conservation of functions for some isoforms, while also allowing for the generation of new recognition sites and specialized cellular functions. Here we present several crystal structures of the myosin Va or the myosin Vb globular tail domain (GTD) that gives insights into how the motor is linked to the recycling membrane compartments via Rab11 or to the melanosome membrane via recognition of the melanophilin adaptor that binds to Rab27a. The structures illustrate how the Rab11-binding site has been conserved during evolution and how divergence at another site of the GTD allows more specific interactions such as the specific recognition of melanophilin by the myosin Va isoform. With atomic structural insights, these structures also show how either the partner or the GTD structural plasticity upon association is critical for selective recruitment of the motor.

GTPases | DIL motif | Rab effector | intracellular traffic

Directed movement is essential for life, and cytoskeleton-based motors generate mechanical force and motion to precisely organize the cell. Their coordinated actions allow them to play key roles in nearly every physiological process. Class V myosins (Myo5) and the related plant class XI myosins are a group of multifunctional actin-based nanomotors that have evolved from one of the three ancient myosin subfamilies (1). The motor domain and extended lever arm of these myosins is followed by a coiled coil dimerizing region and the C-terminal globular tail domain (GTD) that primarily plays a role in selective cargo recruitment. Little is known, however, about how this GTD sequence has evolved to serve both a role in regulation of the motor activity (2, 3) and specific recruitment of the motor, which is critical to control precisely in space and time when the motor is activated for different cellular functions.

The Myo5 motor acts as a transporter or a tether for a wide variety of membrane cargoes, such as melanosomes of pigment cells, apical recycling endosomes in polarized epithelial cells, as well as recycling endosomes and endoplasmic reticulum tubules into the dendritic spines of neurons to support synaptic plasticity (4). There are three Myo5 isoforms, Myo5A–C, in vertebrates, and all three isoforms can exist in different alternative splice variants (5, 6). Mutations in Myo5A and Myo5B lead, respectively, to the rare neurological disease Griscelli syndrome type I (7) and to an epithelial disorder called "microvillus inclusion disease" (8).

Rab GTPases play critical roles in the recruitment of Myo5 motors to their cellular cargo (6, 9). They act as regulated molecular switches and the GTP-bound active conformation recruits effector proteins that operate specifically for different membrane traffic steps (10). Whereas some Rabs such as Rab11 interact directly with Myo5A and Myo5B GTDs, other Rabs bind indirectly through adaptors. The Rab27 effector melanophilin (MLPH) interacts with Myo5A (11); Rab11-FIP2—an effector of Rab11—also directly binds to Myo5B (12).

Interestingly, Rab-mediated Myo5 recruitment has been evolutionarily conserved for Rab11. The yeast Myo5 Myo2p transports secretory vesicles via a Rab GTPase cascade involving Ypt31/32 and Sec4 (Rab11 and Rab8 homologs, respectively) (13), and in *Drosophila*, Myo5 also binds Rab11 to drive secretory vesicle movement (14). In contrast, there are Myo5 isoform-specific interactions between the GTD and specialized adaptors, such as Myo5A association with MLPH. High-resolution structural data are essential to understand how the GTD sequence diverged among isoforms during evolution to maintain core shared functions while promoting diversification of cellular roles by acquiring new specific partner interactions.

We are focusing on the GTD-mediated Myo5 recruitment by direct interaction with Rab11, which plays important roles for recycling cellular pathways and in its recruitment by interaction with MLPH for Rab27-associated melanosome transport. The first structures of the Myo5A–GTD and its complex with two cargo molecules (RILPL2 and the 26-residue peptide MLPH–globular tail binding domain (GTBD) have been reported recently at 2.5- and 2.4-Å resolution, respectively (15). We present here higher resolution (1.9 Å and 1.5 Å) structures of the Myo5A–GTD and the Myo5A–GTD:MLPH–GTBD complex and also structures of the Myo5B–GTD in complex with the active and inactive states of Rab11. These structures provide the molecular basis for describing both evolutionarily conserved and specialized recruitment of Myo5 and they highlight the role of

Significance

Directed movement is essential for life, and cytoskeleton-based motors generate mechanical force and motion to precisely organize the cell. Their selective recruitment and activation at particular times and positions in cells is critical to numerous cell processes. This paper provides unique insights into the specific recognition of cellular compartments by the myosin V nanomotor via direct or indirect interactions with Rab GTPases. These studies highlight the role of plasticity in the binding site to achieve selectivity in cargo/motor recognition. We also describe how the globular tail domain sequence of the motor diverged among isoforms during evolution to maintain core shared functions while promoting diversification of cellular roles by acquiring new specific partner interactions.

Author contributions: O.P. and A.M.H. designed research; O.P., W.A., C.G., M.L., D.C., B.B., S.H., and P.E. performed research; O.P., M.A.T., P.E., and A.M.H. analyzed data; and O.P. and A.M.H. wrote the paper.

The authors declare no conflict of interest.

*This Direct Submission article had a prearranged editor.

Data deposition: The atomic coordinates and structure factors have been deposited in the Protein Data Bank, www.pdb.org (PDB ID codes 4LWZ, 4LX0, 4LX1, and 4LX2).

[1]To whom correspondence may be addressed. E-mail: anne.houdusse@curie.fr or Olena.Pylypenko@curie.fr.

This article contains supporting information online at www.pnas.org/lookup/suppl/doi:10.1073/pnas.1314329110/-/DCSupplemental.

induced fit to promote selective cargo/motor recognition essential for specialized Myo5 functions.

Results and Discussion

Isoform-Specific Structural Differences of the Myo5 GTD and Conservation Upon Evolution. Cellular compartment organization and dynamic cell trafficking is essential for life. For such functions, the recruitment of nanomotors to specific compartments is in large part mediated via direct or indirect interactions with Rab GTPases. We have solved the structure of the human Myo5B GTD bound to active and inactive Rab11a, as well as the structure of the human Myo5A GTD alone and in a complex with the MLPH–GTBD (Table S1). The similarity between the vertebrate Myo5 GTD structures determined here (Fig. 1) strongly suggests that the GTD adopts a well-structured fold with limited flexibility in the relative position of the two subdomains it contains. These structures also indicate that binding of either Rab11 or MLPH to the GTD does not induce major changes in the conformation of the GTD upon binding to these partners. The overall structures of the Myo5A and Myo5B GTDs are very similar (Fig. 1*B*), reflecting the high degree of sequence conservation between different species (Fig. S1). However, the electrostatic distribution on the surface of the GTD differs significantly, in particular on subdomain 1 (SD-1) (Fig. S2). The main structural difference corresponds to the small region, flanked by two strictly conserved prolines, that links the H1 and H2 helices (Fig. 1*C*). The Myo5C sequence similarity with Myo5A is high in this region and in fact is high enough overall to assume that the Myo5A structure is also representative of Myo5C. In the Myo5A structure, several hydrophobic residues belonging to the H1′ helix are exposed on the surface of SD-1. In Myo5B, this region between the H1 and H2 helices is in fact a linker and displays a more polar surface. This surface in SD-1 is thus an isoform-specific interaction site. Interestingly, it has been shown that this region of Myo5A is involved in binding to the isoform-specific adaptor RILPL2 (15) that binds to Rab36 (16).

Comparison of the vertebrate and yeast Myo5 GTD structures (17, 18) defines the core of the GTD as composed of 12 helices subdivided in two closely packed subdomains consisting of alpha-helical bundles that share the long H5 helix (Fig. 1 and Fig. S1*C*). The lengths of several helices and loops vary between the yeast and vertebrate GTDs, indicating that some of the surface of the GTD has been poorly conserved during evolution. This seems to be particularly pronounced for SD-1 for which significant sequence differences limit homology modeling for distant myosins such as the plant myosins. A major difference between the vertebrate Myo5 and yeast Myo2p and Myo4p is also the relative subdomain orientation found for each of these GTDs (Fig. S2*B*). Note that the subdomain orientation is likely important to control how different partners may simultaneously bind to the GTD. Interestingly, the H5–H6 loop in SD-2, which has an important regulatory role in vertebrate Myo5 isoforms, is not conserved in yeast Myo5s (Fig. S1*A*). It contains the serine S1650 in mouse Myo5A, whose phosphorylation by calcium/calmodulin-dependent protein kinase II results in its dissociation from melanosomes (19). In contrast, the insulin-stimulated phosphorylation of the same residue by Akt2 enhances the Myo5A-mediated transport of GLUT4 to the plasma membrane in adipocytes (20). Further studies will be necessary to investigate how the phosphorylation at this regulatory site might control the recruitment of the motor for different cargoes.

Myo5 motor activity is controlled by interactions between the motor domain and its tail. Conserved basic residues (K1706 and K1779) found on the tip of the SD-2 H7–H8 loop and H11 helices are essential for this regulation (21). Whereas this region is conserved in vertebrate Myo5 and yeast Myo2p, it is not in Myo4p (18). Interestingly, the same Myo5 residues are involved in interaction with Sec15—a subunit of the exocyst showing a link between the motor and the tethering complexes (13). It is thus interesting that the SD-2 GTD region involved in both inhibition of the motor and its binding to the exocyst upon activation has been conserved in yeast Myo2p and vertebrate Myo5.

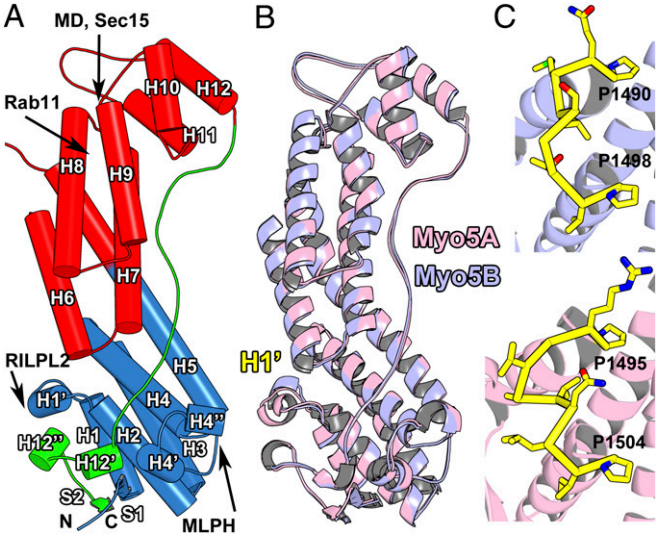

Fig. 1. Crystal structure of the Myo5 GTD. (*A*) Cartoon representation of the Myo5A–GTD structure, SD-1 is highlighted in blue and SD-2 in red, the intersubdomain linker in green. The main characterized binding sites for Rab11, RILPL2, MLPH, Sec15, and MD (motor domain) are indicated with arrows. (*B*) Superimposition of Myo5A and Myo5B GTDs. (*C*) Linker region between H1 and H2 helices; Myo5B (*Upper*) and Myo5A, which contains the H1′ helix (*Lower*).

Conserved Structural Recognition of Myo5–GTD with Rab11 Family Members. The Myo5B:Rab11 interaction is required for recycling of transferrin in nonpolarized cells, in apical membrane trafficking, and de novo lumen formation in polarized epithelial cyst cultures (9). This interaction has been conserved in evolution because binding of the yeast homolog of Rab11, Ypt31/32 to Myo2p, mediates polarized secretion in yeast (22). To understand the molecular basis of the interaction between Rab11 family members and Myo5, we have determined the crystal structures of Myo5B–GTD bound to Rab11 in both active and inactive conformations at atomic resolution.

The Myo5B Rab11-binding site is found on one side of the SD-2 bundle. It is formed mostly by the H8 helix and a few residues of the H9 and H10 helices along with the loop connecting H5 and H6 (Fig. 2). As expected from the high degree of sequence homology between the proteins, the residues of Myo5A and Myo5B involved in Rab11 binding are largely identical (Fig. S1*A*). Interestingly, four residues forming the Rab11-binding site are substituted to nonhomologous ones in the Myo5C sequence (Fig. S1*A*), which explains why Rab11 does not bind to Myo5C (6). The Rab11-binding site is also conserved in yeast Myo2p (Fig. S1*A*), but not in yeast Myo4p, which binds to a different partner, She3p, at this site (18). The secondary structure elements are conserved in this region but seven residues involved in Rab11 interaction differ in the Myo4p sequence compared with that found in the Myo2p and Myo5B sequences. This is sufficient to modify the binding-site specificity (Fig. S1*A*). Whereas it is quite remarkable that the Rab11-binding site is conserved from the yeast Myo2p to vertebrates, sequence comparison of several myosins shows that the Rab11-binding site is not conserved in the more distantly related amoeba Myo5s and plant myosin XIs (Fig. S1*A*), although Rab11 homologs are present (Fig. S3). Further studies are necessary to determine whether Rab11s interact with myosin GTDs in a similar or distinct manner in these organisms.

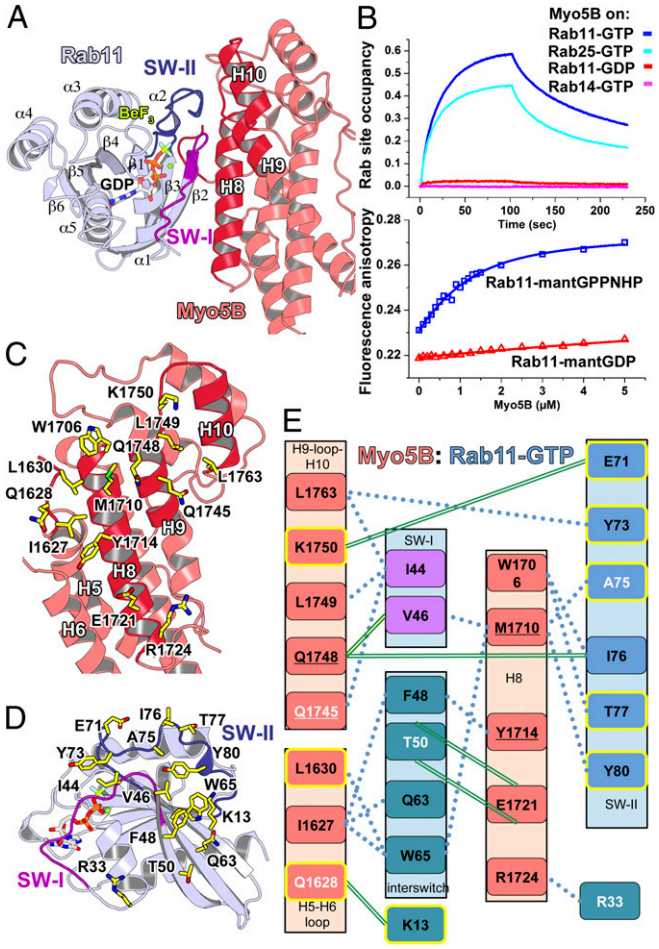

Fig. 2. Crystal structure of Rab11–GTP bound to Myo5B–GTD. (*A*) Overall structure of the complex. (*B*) The *Upper* diagram illustrates the real-time surface plasmon resonance (SPR) analysis of the interaction between GST–Myo5B–GTD (250 nM) and tethered 6× His–Rabs ($K_{dRab11GTP}$ = 254 ± 39 nM, $K_{dRab11GDP}$ = 8,500 ± 1,900 nM, $K_{dRab25GTP}$ = 537 ± 66 nM, Rab14GTP binding is not detected). Fluorescence anisotropy measurements of Myo5B–GTD binding to Rab11:mantGppNHp, K_d = 620 ± 100 nM; or Rab11:mantGDP, K_d = 19,000 ± 2,000 nM are shown below. (*C*) Myo5B residues interacting with the active form Rab11a–GTP. The Myo5B Rab11 binding epitope is formed by two hydrophobic patches surrounded by a few polar residues. (*D*) Rab11–GTP residues involved in Myo5B binding. (*E*) Schematic view of the Rab11–GTP–Myo5B interactions. Mutations in the underlined residues result in Rab binding deficiency (9, 17, 22). Residues conserved between yeast Myo2p and vertebrate Myo5, as well as residues conserved within Rabs, are labeled in black. Hydrophobic contacts are shown as dashed lines, hydrogen bonds as double lines. The switch-1 I44 and the switch-2 Y73 of Rab11 bind to the Myo5B hydrophobic patch formed by residues of the H9 and H10 helices, whereas the other Rab residues bind to the patch formed mostly by residues of the H8 helix. The residues that do not form interactions in the Rab11–GDP to Myo5B interface are highlighted in yellow (see also Fig. S6).

Myo5B Binding Results in Significant Structural Rearrangement of Rab11. The structural basis for the specificity of active Rab binding to selected partners is not fully understood. It is currently assumed that, whereas the inactive form of Rab has rather flexible switches, these would be stabilized in the active form of Rab and specific sequence differences among Rabs would dictate whether or not an active Rab can recruit a partner on a vesicle (23, 24). An active Rab11 binds to the myosin GTDs via the canonical effector recognition site of the GTPases, which includes switch 1, switch 2, and the interswitch region (Fig. 2). Surprisingly Rab11 binds to the Myo5B–GTD with dramatically different conformations of the switches from those in the eight previously determined active Rab11 structures (Fig. 3*A* and Fig. S4*A*). When bound to Myo5B, the switch-2 helix of Rab11 is expanded as a loop with only one turn of a 3_{10} helix, and the N-terminal part of switch 2 hangs over the BeFx ion that mimics the gamma-phosphate moiety of the nucleotide. A ∼1.8-Å shift of switch 1, compared with that found in the previously determined active conformation of Rab11, allows the formation of new specific interactions between the two switches that stabilize this overall conformation of the active site in which the gamma phosphate seems trapped (Fig. S4 *C* and *D*). This is particularly important because this recognition would enhance the lifetime of the active form of the GTPase and thus the maintenance of a high-affinity interaction with the motor, essential for promoting long-range processive transport or tethering by the motor.

The Myo5B binding requires significant remodeling of both Rab11 switches, suggesting that Rab11 binding to the effector might involve an induced fit mechanism. Note that some Rab11 switch-2 structural plasticity has already been reported as being important for the binding of some effectors (25). However, the remodeling observed here for Rab11–GTP bound to Myo5B is much larger (Fig. S4*A*). The active Rab11 structures have revealed a particular structural organization of the switches and the hydrophobic triad, which differs from that found for other Rab active forms (Fig. S5) and has been suggested to be a main determinant for Rab/effector binding specificity (24) (Fig. 3*B* and Fig. S5). Surprisingly, the Rab11:Myo5B structures we determined show that Myo5B association requires significant conformational rearrangements of both switch 1 and switch 2, in which the Thr67 conformation plays a pivotal role (Fig. 3*C*). Interestingly, Myo5B binding promotes a conformation of the active GTPase that shares similarities with that seen for the majority of Rabs in their active state (Fig. S5). Moreover, the Rab11 residues directly involved in Myo5 binding are conserved among most Rab family members (Fig. S3). Whereas Rab25 interacts with the Myo5B GTD with similar affinity as Rab11, others such as Rab14 do not bind (Fig. 2*B*), although Rab14 does bind to the Rab11-binding domain of Rab11–FIP2 (26). The Rab11:Myo5B structure thus illustrates how plasticity in the switch region of Rab proteins is required for the binding of these effectors and thus influences the selectivity of Rab recognition. The sequence of the core of these Rabs is likely to play an even more important role for selectivity of their effector than the exact sequence of the residues involved in binding (27). This illustrates how difficult prediction of selectivity can be and demonstrates the importance of structural and functional studies for these Rab/effector interactions to define which effectors and molecular motors different cellular compartments can actually recruit.

We also obtained a structure of Rab11–GDP bound to Myo5B. The binding only involves switch 1 and the interswitch regions (Fig. S6), whereas switch 2 is mostly disordered, indicating that it is not stable enough to participate in interactions with the GTD. In contrast, switch 1 is stabilized by interactions with the partner that are similar to those found in the Rab11–GTP complex structure (Fig. S4). The complex formation results in the burying of 660 Å^2 of solvent accessible surface area that is significantly less compared with 1,027 Å^2 in the Myo5B:Rab11–GTP. Consistent with these observations, we found that Myo5B–GTD binds Rab11–GTP with higher affinity than Rab11–GDP (Fig. 2*B*). The high stability of the Myo5B:Rab11–GTP complex and the fact that the complex traps the gamma-phosphate (Fig. S4*C*) appears consistent with the ability of the motor to carry its cargo via this direct interaction. Importantly, the avidity of Myo5B in the cellular compartment is further enhanced by its dimerization, allowing it to interact simultaneously via two Rab-binding sites thus increasing the probability that it remains bound during cargo transport and tethering.

Rab11 and Myo5B can both interact with Rab11–FIP2 (12) and further studies are necessary to define the stoichiometry and structure of the tripartite complex. In response to a Ca^{2+} flux, Myo5B is recruited to the recycling endosome-associated Rab11:

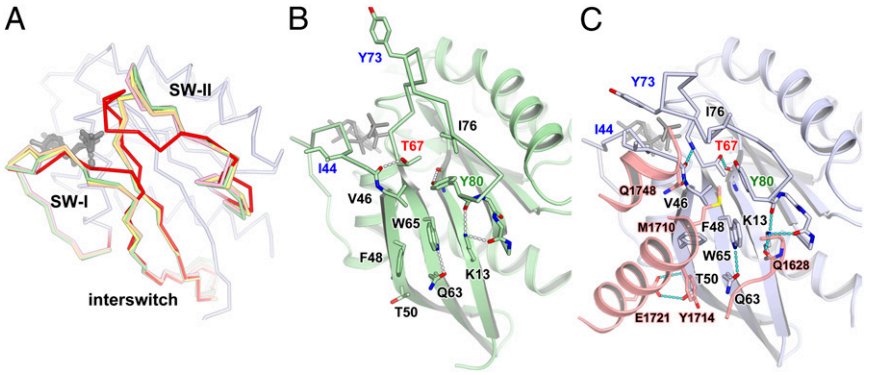

Fig. 3. Structural rearrangement of the Rab11 switches is required to bind to Myo5B. (*A*) Rab11 isoforms unbound structures in the GTP bound state [Protein Data Bank (PDB) codes: 1OIX, 1YZK, 2F9M, and 1OIW] exhibit well-ordered switches with a very similar conformation (pale colors). Both Rab11–GTP switches undergo significant rearrangement upon Myo5B binding (red). (*B*) Description of the specific interactions stabilizing the unbound active Rab11 structures. The T67 residue (red) forms an H bond with the G45 that results in a slight bulge of the switch-1 I44 residue (blue). The space between the switch-2 helix and the surface of the beta-sheet is occupied by the Y80 side chain (part of the hydrophobic triad) that forms an H bond with the carbonyl of L16. The conserved hydrophobic residues I44 and Y73 from switch 1 and switch 2 are thus spaced far apart. (*C*) In the Myo5B-bound Rab11–GTP structure, T67 (red) interacts with the main chain oxygen of L16. The Thr side chain thus fills the space between the beta-sheet and the switch-2 helix, pushing away the Y80 side chain and drastically changing the conformation of the hydrophobic triad (F48,W65,Y80). Interestingly, an hydrogen bond forms between the switch-1 G45 and switch-2 A68 residues maintaining the two switches close together, and this promotes the formation of a hydrophobic patch on the surface of Rab11 by aligning the conserved hydrophobic residues I44 and Y73 so that they interact with a complementary hydrophobic patch on the surface of Myo5B. The observed Rab11 conformation is similar to what is observed for most Rab GTPases in their active state to promote effector binding. It drastically differs from the previously observed conformation for active Rab11 unbound or bound to effectors (described in Fig. S5*B*).

Rab11–FIP2 complex and drives AMPA receptors trafficking to synaptic sites (28). The Rab11:Rab11–FIP2 and Rab11:Myo5B structures demonstrate that Rab11 binds to these effectors using the same binding site (Fig. S7), although Rab11 exploits its conformational plasticity to bind these effectors with different structures and affinities. It is not known whether independent Rab11:Rab11–FIP2 and Rab11:Myo5B complexes can form at the surface of the cargo to be transported. Because the Myo5B GTD also directly interacts with Rab11–FIP2 (12), it is likely that the three proteins also interact in a tripartite complex. More studies are necessary to elucidate how direct interactions between Myo5B and Rab11–FIP2 form and whether they are compatible with direct interactions of Rab11 with Myo5B. Interactions with Rab11–FIP2 are not only likely to strengthen the binding of the motor and maintain its active conformation, they can also influence its function in cells by tethering the motor to the plasma membrane via interaction of the C2 domain of Rab11–FIP2 with phospholipids (29).

Structural Recognition of the MLPH by an Isoform-Specific Binding Site of the Myo5A–GTD. The Rab11 binding site on the GTD has been highly conserved among some isoforms, whereas other binding regions of the GTD have evolved to confer a unique function for a given isoform by promoting selective binding to distinct partners. An example of such specificity is the role that Myo5A plays in melanosome transport in pigmented cells. Myo5A, but not Myo5B or Myo5C, interacts directly with MLPH, which also binds to Rab27 at the surface of melanosomes (30). This tripartite complex links melanosomes to the actin network and mediates short-range transport or tethering, which allows melanosome retention in the periphery and, ultimately, melanosome transfer to keratinocytes (31). This process is fundamental to mammalian skin and hair pigmentation.

MLPH has two independent Myo5A-binding domains (32, 33). The MLPH domain (residues 320–406), that binds the melanosome-specific Myo5A exon-F region upstream of the GTD, appears to be required for Myo5A recruitment to and transport of melanosomes (34) and is thus critical for the specificity of this recruitment. Interestingly, the brain-type Myo5A isoform, lacking exon-F, also binds to MLPH, although with a weaker affinity (32). The second myosin-binding domain involves residues 147–240 of MLPH (32), which directly interacts with the Myo5A GTD but not the Myo5B GTD. The minimal 26-residue GTBD sequence (176–203) directly binds to the GTD with the same affinity as MLPH (33). Myo5A mutations in mice, an animal model for human Griscelli syndrome type 1, result in the "dilute" phenotype, with a lighter coat color and lethal neurological defects (35). Several dilute missense mutations in the GTD of Myo5A impair MLPH binding and indicate a crucial role of the Myo5A–GTD for both melanosome transport and neurological function (36).

The structure of Myo5A–GTD bound to the MLPH GTBD fragment shows that only 7 residues from the middle part of the peptide (residues 185–191) interact specifically with the SD-1 of Myo5A–GTD. Residues 192–196 are poorly stabilized and the rest of the peptide cannot be observed in the electron density map (Fig. S8*A*). The observed Myo5A MLPH-binding site is identical to that visualized in the lower resolution structure of the complex (15), but the peptide side chain conformations and the stabilizing interactions are slightly different. The MLPH peptide binds in the cleft formed between the H3 and H5 helix and involves a loop preceding the H5 helix (Fig. 4*A*). This region, which is mostly conserved in the sequence of the three vertebrate Myo5 isoforms, is structurally different in the yeast Myo5 homologs (Fig. 4*B*), indicating that it has evolved and acquired binding properties to mediate a specific role in vertebrate Myo5s. Despite its very small size, the MLPH peptide makes extensive contacts with the Myo5A GTD (Fig. S8*A*). Whereas several interactions involve the peptide backbone, there are also more specific interactions involving residues F191, L189, R187, and K186. The MLPH GTBD has a characteristic charge distribution, and charged residues on either side of the ordered bound peptide residues contribute significantly to binding and possibly orientation of MLPH via charge complementarity with the GTD surface (Fig. S8 *B* and *C*).

Local Plasticity on the GTD Contributes to Specificity of the Myo5A–GTD MLPH Recognition. Comparison between the apo–Myo5A and the MLPH–Myo5A structures reveals that the GTD undergoes conformational rearrangements upon MLPH binding, involving mainly Y1596. The hydrophobic cleft between the H3 and H5 helices is not as deep in the apo–Myo5A structure because the side chain of Y1596 is oriented toward the surface of the protein, exposing the hydroxyl group on the surface. This orientation fills the space between the helices (Fig. 4*E*). In the MLPH-bound state, the Y1596 side chain is oriented toward the interior of the protein and is stabilized by a hydrogen bond (Fig. 4*E*). The hydrophobic cleft can then accommodate the hydrophobic anchoring residues from MLPH. The bound MLPH F191 together with the Myo5A Y1596 and F1562 side chains form a cluster of aromatic residues of extended ladder type (37), stabilizing the complex.

Myo5B–GTD binds the MLPH–GTBD peptide with very low affinity (15). This GTD has a very similar structure for the region corresponding to the MLPH-binding site in Myo5A, but exhibits

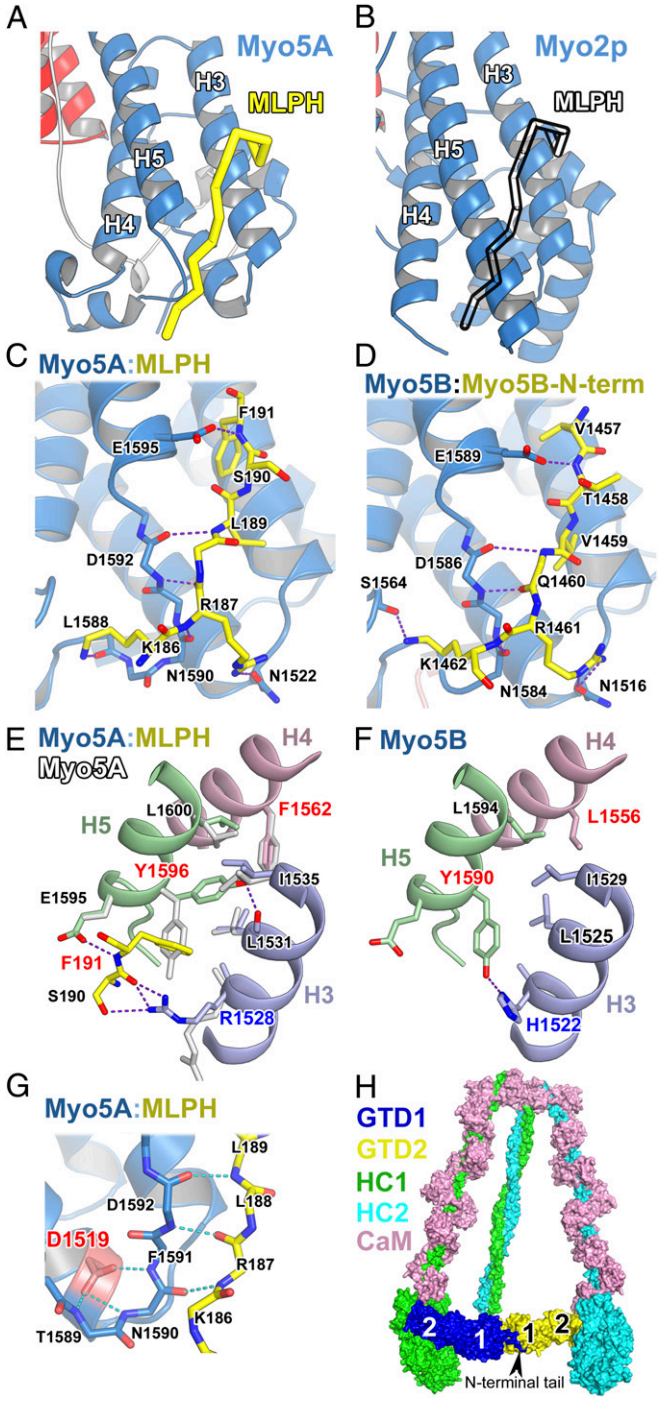

Fig. 4. Binding of MLPH to Myo5A GTD. (*A*) The MLPH GTBD (yellow) binding site is located within SD-1 (blue) of Myo5A GTD. (*B*) The Myo2p structure is not compatible with a peptide ligand binding at the same site. (*C*) Two MLPH hydrophobic residues, F191 and L189, are anchored into the hydrophobic cleft of the Myo5A–GTD identified between the H3 and H5 helices. In addition, the MLPH main chain is stabilized by multiple polar interactions with myosin. The side chains of E1595 from the H5 helix and R1528 from the H3 helix capture the peptide backbone from both sides by forming hydrogen bonds (see also *E*). The MLPH residues 187–189 and the Myo5A residues 1590–1592 form a hydrogen-bonding network corresponding to a parallel beta-structure. The side chains of positively charged residues K186 and R187 make hydrogen bonds to the L1588 carbonyl group and the N1590 and N1522 side chains, respectively. (*D*) The N-terminal tail of Myo5B from a symmetry-related molecule makes interactions in the hydrophobic site found between helices H3 and H5 in a manner similar to that observed in the Myo5A:MLPH complex but the directionality of the peptide bound in the cleft is opposite. (*E*) Structural rearrangements of the Myo5A–GTD upon MLPH binding. Local conformational changes of Myo5 residues Y1596 and R1528 are necessary to accommodate the MLPH peptide in its binding pocket. The apo–Myo5A is shown in white and the Myo5A in the complex is colored. (*F*) Same region as found in the Myo5B structure. Differences in the sequence of core residues in particular L1556 contribute to destabilize the Y1590 conformation necessary for MLPH binding. (*G*) The D1519 residue, mutated to glycine in Griscelli syndrome, stabilizes the MLPH-binding loop conformation. (*H*) Model of the off-state of Myo5B, indicating how each N-terminal tail of a GTD could interact with the SD-1 region ("MLPH" binding site) of the other GTD in the dimer and could stabilize the folded conformation as well as mask interaction with partners. GTD subdomains are labeled with numbers.

small yet critical differences. The Y1590 orientation is similar to that of the apo–Myo5A structure and is stabilized in Myo5B by a hydrogen bond with H1522, which substitutes for the R1528 of Myo5A (Fig. 4*F*). The structural transition to open the binding pocket might thus be less favored in Myo5B. Also, the shorter histidine side chain cannot stabilize the binding of MLPH as the arginine does in Myo5A. In addition, the substitution of the F1562 residue by L1556 in Myo5B changes the hydrophobic pocket in the GTD and results in poorer peptide stabilization because the extended ladder interaction cannot be formed. There are two more substitutions (F1512Y and V1515I) in the Myo5B core that may change the site plasticity preventing its opening. The binding site occupied by MLPH in Myo5A is, however, relatively conserved in other vertebrate Myo5 isoforms, and the interactions that occur via the peptide backbone may also be the basis for the recognition of other peptides. In the Myo5B structure, the binding site is in fact occupied by the N-terminus extension of a symmetry-related GTD, and the observed interactions are very similar to that formed in the Myo5A:MLPH complex (Fig. 4*D*). It is thus likely that this region also corresponds to a functional binding site for other Myo5 isoforms for peptides of different sequences.

Three dilute mutations (I1510N, M1513K, and D1519G) of Myo5A–GTD (36) are located in the H2 helix within SD-1. The two residues, I1510 and M1513, are packed in the protein hydrophobic core and their substitution to polar residues might result in the misfolding or destabilization of the SD-1 structure. Quite remarkably, D1519 directly stabilizes the MLPH-binding loop preceding H5 via hydrogen bonds to the main chain nitrogens of residues 1589–1591 (Fig. 4*G*). This specific mutation thus directly validates the MLPH-binding site described here and demonstrates the role of the GTBD of MLPH in the Myo5A motor recruitment for melanosome transport. Light neurological impairment has also been described for the missense I1510N mutation and when the last eight residues of the Myo5A–GTD are missing in dilute mice (36).

Mutational analysis has shown that the SD-2 tip of the GTD interacts with the motor domain in the folded inhibited state (21). The general topology of the folded Myo5 conformation indicates that the SD-1 tips of the two GTDs in the folded Myo5 dimer might interact with each other and with the stalk. Interestingly, the interactions of the N-terminal tail of the Myo5B GTD with the SD-1 region of a neighboring molecule (Fig. 4*D*) might represent stabilizing interactions of the "off-state" of Myo5 (Fig. 4*H*). This SD-1 region is in fact the binding site for the MLPH GTBD (Fig. 4 *C* and *D*). Whereas the MLPH GTBD has low binding affinity for the inhibited Myo5A, it has an effect on activation of its ATPase activity (38). This is consistent with the fact that the MLPH GTBD binding site is not exposed in the folded Myo5. Binding of MLPH to Myo5A likely first occurs via the recognition of the Myo5A exon-F surface only. These interactions could destabilize the motor off-state, making the GTD MLPH binding site more accessible. Then, the MLPH GTBD might reach its binding site and this would prevent Myo5A from

BIOCHEMISTRY

reforming interactions with the head and folding back in the off-state. The Myo5A–GTD interactions with MLPH thus play an important role in sustaining activation of the motor. This mechanism supports the previously proposed hypothesis that the physiologically relevant activation pathway involves binding of cargo-receptor proteins to the motor (39, 40).

Conclusions

Our structural results provide important insights into how local plasticity contributes to binding of myosins to their partners and how differences in this plasticity among myosin isoforms or partners can contribute to selective recognition of a motor for its cargo. We have observed and defined two different binding sites on the GTD that allow specific recruitment of the motor and how these have been conserved in evolution. Conservation of some features in the yeast and vertebrate Myo5 SD-2 allows recognition of both the active and inactive Rab11 conformations with different affinities. Surprisingly we find that the high-affinity Rab11–GTP binding to Myo5 requires substantial structural plasticity in the Rab partner, which is likely important to define the specificity of binding of different Rab GTPases. The vertebrate Myo5 SD-1 has evolved to form an isoform-specific binding site for partners. Minor differences in the SD-1 sequence modulate local Myo5A conformational flexibility and define selectivity of the binding site toward the MLPH GTBD. Whereas the precise sequence of the residues involved in the binding site is important, these structures show that strong and isoform-specific recognition of Rabs by Myo5 and of Myo5 GTD isoforms by MLPH is controlled by how easily local rearrangements can occur at the binding interface. These structural insights highlight the unsuspected role of core residues either in the myosin GTD or in its partner to precisely tune specificity of recognition between a motor and its partner.

Materials and Methods

All proteins used in this study were expressed in *Escherichia coli*. Crystals were obtained by the hanging drop vapor diffusion method. Detailed methods describing protein preparation, crystallization, structure determination, and biochemical assays can be found in *SI Materials and Methods*.

ACKNOWLEDGMENTS. We thank Pierre Legrand, Beatriz Guimares, and Andrew Thompson for their assistance with beamline Proxima-1 at the Soleil synchrotron and for their constant support. This work was supported by Association pour la recherche contre le cancer Grant SFI20121205398, a Fondation pour la recherche medicale équipe 2010 grant and the Agence nationale de la recherche BLAN 2010 121201 (to A.M.H.) as well as National Science Foundation MCB-1244235 Grant (to M.A.T.). This work has been done by a team (A.M.H.) belonging to the labex CelTisPhyBio 11-LBX-0038.

1. Richards TA, Cavalier-Smith T (2005) Myosin domain evolution and the primary divergence of eukaryotes. *Nature* 436(7054):1113–1118.
2. Liu J, Taylor DW, Krementsova EB, Trybus KM, Taylor KA (2006) Three-dimensional structure of the myosin V inhibited state by cryoelectron tomography. *Nature* 442(7099):208–211.
3. Thirumurugan K, Sakamoto T, Hammer JA, 3rd, Sellers JR, Knight PJ (2006) The cargo-binding domain regulates structure and activity of myosin 5. *Nature* 442(7099): 212–215.
4. Hammer JA, Sellers JR (2012) Walking to work: Roles for class V myosins as cargo transporters. *Nat Rev Mol Cell Biol* 13(1):13–26.
5. Seperack PK, Mercer JA, Strobel MC, Copeland NG, Jenkins NA (1995) Retroviral sequences located within an intron of the dilute gene alter dilute expression in a tissue-specific manner. *EMBO J* 14(10):2326–2332.
6. Roland JT, Lapierre LA, Goldenring JR (2009) Alternative splicing in class V myosins determines association with Rab10. *J Biol Chem* 284(2):1213–1223.
7. Pastural E, et al. (1997) Griscelli disease maps to chromosome 15q21 and is associated with mutations in the myosin-Va gene. *Nat Genet* 16(3):289–292.
8. Ruemmele FM, et al. (2010) Loss-of-function of MYO5B is the main cause of microvillus inclusion disease: 15 novel mutations and a CaCo-2 RNAi cell model. *Hum Mutat* 31(5):544–551.
9. Roland JT, et al. (2011) Rab GTPase-Myo5B complexes control membrane recycling and epithelial polarization. *Proc Natl Acad Sci USA* 108(7):2789–2794.
10. Hutagalung AH, Novick PJ (2011) Role of Rab GTPases in membrane traffic and cell physiology. *Physiol Rev* 91(1):119–149.
11. Fukuda M, Kuroda TS, Mikoshiba K (2002) Slac2-a/melanophilin, the missing link between Rab27 and myosin Va: Implications of a tripartite protein complex for melanosome transport. *J Biol Chem* 277(14):12432–12436.
12. Hales CM, Vaerman J-P, Goldenring JR (2002) Rab11 family interacting protein 2 associates with Myosin Vb and regulates plasma membrane recycling. *J Biol Chem* 277(52):50415–50421.
13. Jin Y, et al. (2011) Myosin V transports secretory vesicles via a Rab GTPase cascade and interaction with the exocyst complex. *Dev Cell* 21(6):1156–1170.
14. Li BX, Satoh AK, Ready DF (2007) Myosin V, Rab11, and dRip11 direct apical secretion and cellular morphogenesis in developing Drosophila photoreceptors. *J Cell Biol* 177(4):659–669.
15. Wei Z, Liu X, Yu C, Zhang M (2013) Structural basis of cargo recognitions for class V myosins. *Proc Natl Acad Sci USA* 110(28):11314–11319.
16. Matsui T, Ohbayashi N, Fukuda M (2012) The Rab interacting lysosomal protein (RILP) homology domain functions as a novel effector domain for small GTPase Rab36: Rab36 regulates retrograde melanosome transport in melanocytes. *J Biol Chem* 287(34):28619–28631.
17. Pashkova N, Jin Y, Ramaswamy S, Weisman LS (2006) Structural basis for myosin V discrimination between distinct cargoes. *EMBO J* 25(4):693–700.
18. Heuck A, et al. (2010) The structure of the Myo4p globular tail and its function in ASH1 mRNA localization. *J Cell Biol* 189(3):497–510.
19. Karcher RL, et al. (2001) Cell cycle regulation of myosin-V by calcium/calmodulin-dependent protein kinase II. *Science* 293(5533):1317–1320.
20. Yoshizaki T, et al. (2007) Myosin 5a is an insulin-stimulated Akt2 (protein kinase Bbeta) substrate modulating GLUT4 vesicle translocation. *Mol Cell Biol* 27(14): 5172–5183.
21. Li X-D, et al. (2008) The globular tail domain puts on the brake to stop the ATPase cycle of myosin Va. *Proc Natl Acad Sci USA* 105(4):1140–1145.
22. Lipatova Z, et al. (2008) Direct interaction between a myosin V motor and the Rab GTPases Ypt31/32 is required for polarized secretion. *Mol Biol Cell* 19(10):4177–4187.
23. Lee M-TG, Mishra A, Lambright DG (2009) Structural mechanisms for regulation of membrane traffic by rab GTPases. *Traffic* 10(10):1377–1389.
24. Merithew E, et al. (2001) Structural plasticity of an invariant hydrophobic triad in the switch regions of Rab GTPases is a determinant of effector recognition. *J Biol Chem* 276(17):13982–13988.
25. Eathiraj S, Mishra A, Prekeris R, Lambright DG (2006) Structural basis for Rab11-mediated recruitment of FIP3 to recycling endosomes. *J Mol Biol* 364(2):121–135.
26. Kelly EE, et al. (2010) Class I Rab11-family interacting proteins are binding targets for the Rab14 GTPase. *Biol Cell* 102(1):51–62.
27. Mishra A, Eathiraj S, Corvera S, Lambright DG (2010) Structural basis for Rab GTPase recognition and endosome tethering by the C2H2 zinc finger of Early Endosomal Autoantigen 1 (EEA1). *Proc Natl Acad Sci USA* 107(24):10866–10871.
28. Wang Z, et al. (2008) Myosin Vb mobilizes recycling endosomes and AMPA receptors for postsynaptic plasticity. *Cell* 135(3):535–548.
29. Lindsay AJ, McCaffrey MW (2004) The C2 domains of the class I Rab11 family of interacting proteins target recycling vesicles to the plasma membrane. *J Cell Sci* 117(Pt 19): 4365–4375.
30. Wu X, Sakamoto T, Zhang F, Sellers JR, Hammer JA, 3rd (2006) In vitro reconstitution of a transport complex containing Rab27a, melanophilin and myosin Va. *FEBS Lett* 580(25):5863–5868.
31. Wasmeier C, Hume AN, Bolasco G, Seabra MC (2008) Melanosomes at a glance. *J Cell Sci* 121(Pt 24):3995–3999.
32. Fukuda M, Kuroda TS (2004) Missense mutations in the globular tail of myosin-Va in dilute mice partially impair binding of Slac2-a/melanophilin. *J Cell Sci* 117(Pt 4): 583–591.
33. Geething NC, Spudich JA (2007) Identification of a minimal myosin Va binding site within an intrinsically unstructured domain of melanophilin. *J Biol Chem* 282(29): 21518–21528.
34. Wu XS, et al. (2002) Identification of an organelle receptor for myosin-Va. *Nat Cell Biol* 4(4):271–278.
35. Mercer JA, Seperack PK, Strobel MC, Copeland NG, Jenkins NA (1991) Novel myosin heavy chain encoded by murine dilute coat colour locus. *Nature* 349(6311):709–713.
36. Huang JD, et al. (1998) Molecular genetic dissection of mouse unconventional myosin-VA: Tail region mutations. *Genetics* 148(4):1963–1972.
37. Lanzarotti E, Biekofsky RR, Estrin DA, Marti MA, Turjanski AG (2011) Aromatic-aromatic interactions in proteins: Beyond the dimer. *J Chem Inf Model* 51(7):1623–1633.
38. Li X-D, Ikebe R, Ikebe M (2005) Activation of myosin Va function by melanophilin, a specific docking partner of myosin Va. *J Biol Chem* 280(18):17815–17822.
39. Sellers JR, Thirumurugan K, Sakamoto T, Hammer JA, 3rd, Knight PJ (2008) Calcium and cargoes as regulators of myosin 5a activity. *Biochem Biophys Res Commun* 369(1): 176–181.
40. Sckolnick M, Krementsova EB, Warshaw DM, Trybus KM (2013) More than just a cargo adapter, melanophilin prolongs and slows processive runs of Myosin va. *J Biol Chem* 288(41):29313–29322.